

# TẠP CHÍ KHOA HỌC ĐẠI HỌC ĐỒNG THÁP Dong Thap University Journal of Science

Số Đặc biệt Hội nghị Khoa học tự nhiên Đồng bằng sông Cửu Long lần IV ISSN 0866-7675 | e-ISSN 2815-567X



122N 0866-7672 | 6-122N 5812-261X

DOI: https://doi.org/10.52714/dthu.14.04S.2025.1575

# CHARACTERIZING COSMIC MUON FLUX AS A FUNCTION OF ZENITH ANGLE USING GEIGER-MÜLLER COINCIDENCE SETUP

Lin-Dan Lieu<sup>1,2,\*</sup>, Thuy-Duyen Pham<sup>1,2</sup>, Phuong-Vy Vo<sup>1,2</sup>, Tan-Loc Huynh<sup>1,2</sup>, Minh-Quan Cao-Dinh<sup>1,2</sup>, Duc-Manh Nguyen<sup>3</sup>, Hong-Duyen Trinh-Tran<sup>1,2</sup>, and The-Thuong Nguyen<sup>4</sup>

<sup>1</sup>Laboratory of Laser Technology, Faculty of Applied Science, Ho Chi Minh City University of Technology (HCMUT), Ho Chi Minh City, 72409, Vietnam

<sup>2</sup>Vietnam National University Ho Chi Minh City, Ho Chi Minh City 71308, Vietnam <sup>3</sup>Equipment, Military Hospital 175, Ho Chi Minh City 72518, Vietnam

<sup>4</sup>Military Science and Training, Military Hospital 175, Ho Chi Minh City 72518, Vietnam

 $*Corresponding\ author,\ Email:\ dan.lieulin@hcmut.edu.vn$ 

Article history

Received: 30/5/2025; Received in revised form: 28/6/2025; Accepted: 06/7/2025

### **Abstract**

The study uses a low-cost, dual Geiger-Müller (GM) tubes coincidence detection device in an outdoor environment to evaluate the relationship between cosmic muon flux on zenith angle. Coincidence occurrences decreased from 484 counts at vertical alignment to 47 counts at horizontal alignment, with zenith angles of  $0^{\circ}$ ,  $30^{\circ}$ ,  $45^{\circ}$ ,  $60^{\circ}$ , and  $90^{\circ}$ . Under normal values at sea level, the measured directional muon flux at  $0^{\circ}$  was 1.301 muons/cm²/min. An exponent of  $n=1.063\pm0.107$  was obtained by fitting the angular dependency to a cosine power law via a Bayesian Markov Chain Monte Carlo (MCMC) approach. The result indicates a qualitative agreement with a cosine-based angular distribution under practical constraints, despite the fact that this value is less than the theoretical expectation ( $n\approx2$ ). The setup achieved a Noise Rejection Ratio (NRR) of 0.373% and a Directional Index (DI) of 0.804, indicating moderate directional selectivity and noise suppression. This study demonstrates the viability of Geiger-Müller detectors in basic cosmic ray research and educational contexts.

**Keywords:** Coincidence counts, cosmic ray muons, Geiger-Müller detector, muon flux, zenith angle.

Cite: Lieu, L. D., Pham, T. D., Vo, P. V., Huynh, T. L., Cao, D. M. Q., Nguyen, D. M., Trinh, T. H. D., & Nguyen, T. T. (2025). Characterizing cosmic muon flux as a function of zenith angle using Geiger-Müller coincidence setup. *Dong Thap University Journal of Science*, 14(04S), 147-161. https://doi.org/10.52714/dthu.14.04S.2025.1575

Copyright © 2025 The author(s). This work is licensed under a CC BY-NC 4.0 License.

## ĐẶC TRƯNG CỦA THÔNG LƯỢNG MUON TRONG VŨ TRỤ NHƯ MỘT HÀM CỦA GÓC THIÊN ĐỈNH SỬ DỤNG THIẾT LẬP TRÙNG HỢP GEIGER-MÜLLER

Liêu Lin Đan<sup>1,2,\*</sup>, Phạm Thùy Duyên<sup>1,2</sup>, Võ Phương Vy<sup>1,2</sup>, Huỳnh Tấn Lộc<sup>1,2</sup>, Cao Đình Minh Quân<sup>1,2</sup>, Nguyễn Đức Mạnh<sup>3</sup>, Trịnh Trần Hồng Duyên<sup>1,2</sup> và Nguyễn Thế Thường<sup>4</sup>

<sup>1</sup>Phòng thí nghiệm Công nghệ Laser, Khoa Khoa học Ứng dụng, Trường Đại học Bách khoa Thành Phố Hồ Chí Minh (HCMUT), Thành Phố Hồ Chí Minh, 72409, Việt Nam

 $^2$ Đại học Quốc gia Thành phố Hồ Chí Minh, Thành Phố Hồ Chí Minh, 71308, Việt Nam

<sup>3</sup>Khoa Trang bị, Bệnh viện Quân Y 175, Thành Phố Hồ Chí Minh, 725185, Việt Nam

<sup>4</sup>Phòng Khoa học Quân sự và Đào tạo, Bệnh viện Quân Y 175, Thành Phố Hồ Chí Minh, 725185, Việt Nam

\*Tác giả liên hệ, Email: dan.lieulin@hcmut.edu.vn

Lịch sử bài báo

Ngày nhận: 30/5/2025; Ngày nhận chỉnh sửa: 28/6/2025; Ngày duyệt đăng: 06/7/2025

### Tóm tắt

Nghiên cứu này sử dụng một thiết bị phát hiện trùng hợp (coincidence detection) gồm hai ống Geiger-Müller (GM) giá rẻ trong môi trường ngoài trời để đánh giá mối quan hệ giữa thông lượng muon vũ trụ và góc thiên đỉnh. Số lần trùng hợp giảm từ 484 đếm ở vị trí thẳng đứng xuống còn 47 đếm ở vị trí nằm ngang, tương ứng với các góc thiên đỉnh  $0^{\circ}$ ,  $30^{\circ}$ ,  $45^{\circ}$ ,  $60^{\circ}$  và  $90^{\circ}$ . Phù hợp với các giá trị thông thường ở mực nước biển, thông lượng muon theo phương thẳng đứng ( $0^{\circ}$ ) đo được là 1.301 muon/cm²/phút. Khi khớp dữ liệu góc với hàm mũ của hàm cos bằng phương pháp Bayesian Markov Chain Monte Carlo (MCMC), giá trị số mũ thu được là  $n=1,063\pm0,107$ . Kết quả này cho thấy sự phù hợp định tính với phân bố góc dựa trên hàm cos, mặc dù giá trị n thấp hơn so với lý thuyết ( $n\approx 2$ ). Hệ thống đạt được tỷ lệ khử nhiễu (NRR) là 0,373% và chỉ số định hướng (DI) là 0,804, cho thấy mức độ chọn lọc hướng và khử nhiễu vừa phải. Nghiên cứu chứng minh tính khả thi của việc sử dụng ống Geiger-Müller trong nghiên cứu cơ bản về tia vũ trụ và trong bối cảnh giáo dục.

**Từ khóa:** Góc thiên đỉnh, máy dò Geiger-Müller, muon tia vũ trụ, phát hiện trùng hợp, thông lượng muon.

### 1. Introduction

Cosmic ray muons, high-energy particles produced from the decay of pions in the upper atmosphere, are a key component of secondary cosmic radiation (Gaisser, 1990). These muons penetrate the Earth's atmosphere and reach sea level with a flux of approximately  $1 \, muon/cm^2/min$  for a horizontal detector (Arcani et al., 2024). Their flux varies with zenith angle, primarily following a  $cos^2\theta$  dependence due to atmospheric absorption and geometric effects (Borja et al., 2022). Measuring muon flux provides insights into cosmic ray interactions, atmospheric physics, and particle detection technologies (Gaisser, 1990). The use of Geiger-Müller (GM) tubes for muon detection is advantageous due to their simplicity, cost-effectiveness, and reliability in outdoor environments (Bae et al., 2021). Understanding muon flux variations is critical for applications in cosmic ray research, radiation monitoring, and educational experiments.

This study evaluates the zenith angle dependence of cosmic ray muon flux utilizing an outdoor Geiger-Müller (GM) system setup. Specifically, it quantifies muon flux at zenith angles ranging from 0° to 90° over a period of five days, with particular emphasis on angles of  $0^{\circ}$ ,  $30^{\circ}$ ,  $45^{\circ}$ ,  $60^{\circ}$ , and  $90^{\circ}$ ; to validate the  $\cos^2\theta$  dependence model through empirical data. It also assesses the efficacy of a cost-effective GM system for outdoor muon detection. Muon detection systems employing GM tubes have been extensively utilized in educational experiments and semi-professional research due to their simplicity, affordability, and capability to function outdoors (Axani et al., 2017; Arcani et al., 2024). Concurrently, numerous studies have established the correlation between muon flux and zenith angle, demonstrating that the angular distribution adheres to a power law of  $cos(\theta)$ , with an ideal exponent n≈2 at sea level (Gaisser, 1990; Grieder, 2001; Bae et al., 2021; Borja et al., 2022). However, most investigations quantifying muon angles have employed dedicated detectors such as scintillators or Resistive Plate Chambers (RPC), while GM tube-based systems have seldom been utilized for quantifying angular patterns. Notably, no study has applied Bayesian methods, such as Markov chain Monte Carlo (MCMC) simulation, to estimate angular parameters from experimental data collected by the GM system. This gap necessitates an evaluation of the GM measurement system's capability not only at a qualitative level but also through quantitative indicators such as the slope n, the Noise Rejection Ratio (NRR), and the Directional Index (DI). This study aims to address this gap by deploying an outdoor coincident GM system, collecting muon flux data under the zenith angle, and analyzing it using a Bayesian method to verify the fit with the theoretical model.

### 2. Theoretical overview

### 2.1. Muon properties and detection

The muon is an elementary particle resembling the electron, possessing a single negative electric charge and a spin of 1/2 (Particle Data Group, 2020). It is an unstable subatomic particle with a mean lifetime of  $2.2 \,\mu s$ , significantly shorter than that of a free neutron (about 15 minutes), a free proton (at least  $6.6 \times 10^{33}$  years), or an electron, whose lifetime is also possibly infinite (Particle Data Group, 2020; Gaisser, 1990). With a mass of  $105.658 \, MeV/c^2$ , the muon is approximately 200 times heavier than an electron, yet exhibits nearly identical electromagnetic interactions, making it a heavier counterpart (Hughes & Kawall, 2001). In materials science, positive muons are of particular interest. When introduced into a material, a positive muon behaves like a lightweight proton, owing to its positive charge and its mass being about one-ninth that of a proton (Cox, 2009). Similar to how a proton can capture an electron to form hydrogen, a muon can form "muonium" by acquiring an electron. Muonium mimics hydrogen's chemical behaviour, making it valuable in studying hydrogen-like behaviour in materials (Nagamine, 2003).

When an intense proton beam interacts with a light-element target, pions are produced, then decaying into muons. These secondary muons form a beam that can be nearly 100% spin polarised, meaning each muon's spin is aligned anti-parallel to its momentum direction. This high degree of polarisation is a fundamental property utilised in muon spin spectroscopy techniques (Gaisser, 1990; Hughes & Kawall, 2001). Once implanted into a material, the muons slow down, and their spin direction begins to precess under the influence of local magnetic fields, such as those from nearby magnetic atoms. This spin behaviour provides detailed insights into the material's internal magnetic environment. Each muon eventually decays with a mean lifetime of  $2.2~\mu s$ , emitting a positron preferentially in the direction of the muon's spin at the moment of decay.

In Figure 1, when a high-energy proton from outer space (primary cosmic ray) collides with molecules in the atmosphere at an altitude of about 10 km, it creates a series of secondary particles such as pions, kaons, and others. The pions and kaons then decay into muons.

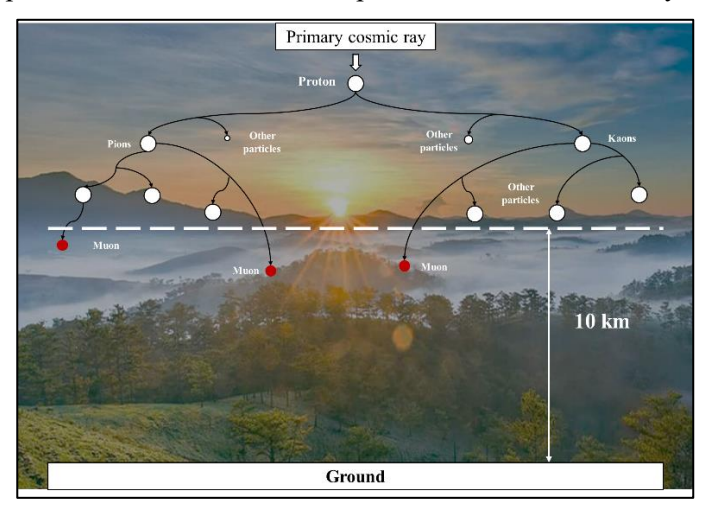


Figure 1. Mechanism of formation and transmission to the ground of muons from primary cosmic rays (CERN, 2023)

### 2.2. Dependence of muon flux on zenith angle

At the ground level, the angle at which cosmic ray muons enter the atmosphere, particularly the zenith angle, has a significant impact on the detection rate. As this angle increases, muons must traverse a greater thickness of the Earth's atmosphere. This extended path results in increased ionisation energy loss and a higher probability of decay before reaching the surface (CAEN S.p.A., 2023). About the zenith angle, muon flux exhibits a cosine power-law dependence, as supported by both theoretical models and experimental data. This relationship can be mathematically expressed as equation (1) (Grieder, 2001a/2001b/2001c):

$$N(\theta) = N(0^{\circ}) \times \cos^{n}(\theta), \tag{1}$$

where  $N(\theta)$  is the muon count at the angle  $\theta$ ,  $N(0^{\circ})$  is the vertical count, and n is an exponent influenced by muon energy and atmospheric thickness. For typical sea-level muons (few-GeV range), n is approximately 2 (ibid).

This angular variation offers a robust method to verify detector performance and alignment. By measuring muon count rates at different zenith angles, such as comparing vertical 0° to 90° orientations, detector sensitivity can be assessed (Bae et al., 2024). With the

 $\cos^2(45^\circ) = 0.5$ , the count rate should be approximately half that of the vertical, assuming consistent environmental conditions and detector settings (Borja et al., 2022).

Figure 2 illustrates the concept of cosmic ray detection with a focus on the zenith angle. It depicts a primary particle (represented by a purple dot) entering the atmosphere, producing a shower of secondary particles (orange lines) that travel toward the ground. A blue curved line represents the trajectory of one such secondary particle, likely a muon, moving from the primary particle to the detector. The detector is implied to be at ground level, where the particle shower converges (CERN, 2023).

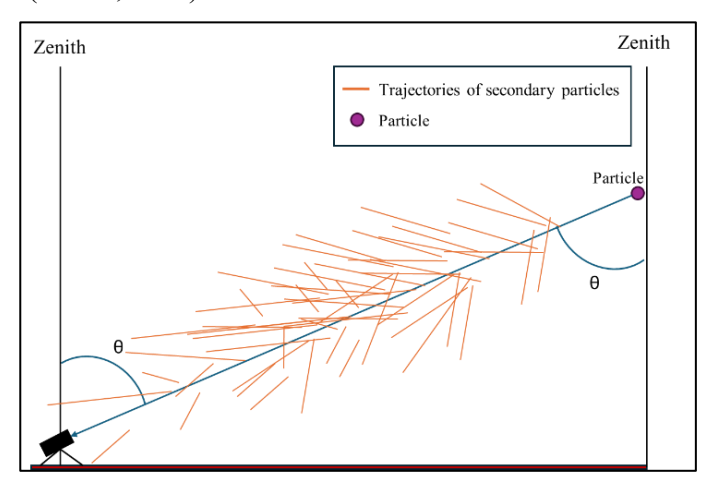


Figure 2. Inclination of the detector concerning the zenithal angle (Arcani et al., 2024)

### 2.3. Detector Configuration

Geiger-Müller (GM) tubes are tools used to detect radiation, like muons. When a muon passes through the tube, it ionizes the gas inside, creating an electrical pulse. Using two or more GM tubes together helps reduce background noise and improves the accuracy of measuring muon direction. This study uses two sets of Geiger-Müller Counter (GMC) circuits, each with a J305 and a J321 tube, as shown in Fig. 3 (from a DIY Kit bought on Aliexpress), along with a coincidence detection (CD) circuit (McKenna, 2021). Each GM tube has a sensitive area of about 10 cm² and runs on a high-voltage supply of 400V. The tubes are placed on a rotational stand to measure muon flow from different angles. The CD circuit makes sure only events detected by both tubes in a set are recorded, cutting down noise from non-muon sources. Data is recorded using a digital counter connected to a microcontroller unit.

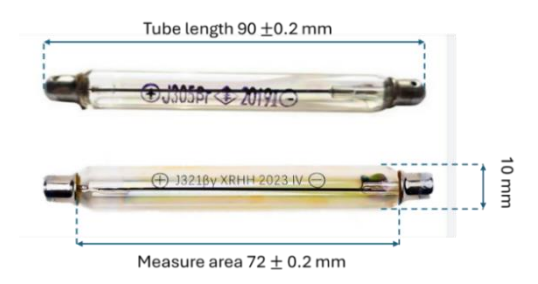


Figure 3. The J305 and J321 GM tubes from the GMC Kit

### 3. Research method

### 3.1. Measuring system and placement

### 3.1.1. DIY GMC system

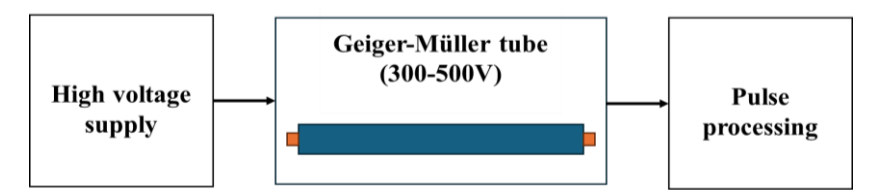


Figure 4. Block diagram of the GMC system

Figure 4 is a block diagram of the GMC system. The high-voltage supply is responsible for generating the high voltage required to operate the GM tube. It takes a low-voltage input, such as from a 5 V power source, and boosts it to a level between 300–500 V. This voltage is essential to create an electric field inside the tube, enabling the detection of ionising particles. Without this block, the GM tube remains inactive. This central block contains the GM tube, which performs the actual detection of radiation. When an ionising particle (such as a cosmic muon or gamma ray) enters the tube, it ionises the gas inside, producing a very short current pulse. This pulse is passed through two key stages. The first is inverter, which converts the current pulse into an inverted voltage pulse for standardisation. Second is the pulse stretcher, which extends the very short pulse (~µs) to a longer pulse (~1.5 ms) to make it usable for output indicators and counting. The stretched pulse will be processed and presented in the form of a Piezo speaker, LED blink, and filter to produce an analog voltage that reflects the overall count rate by the MCU or oscilloscope (Massachusetts Institute of Technology, 2015).

### 3.1.2. Equipment design

The two Geiger-Müller (GM) tubes, designated as GMC1 and GMC2, are separated by a lead layer with a thickness of 3 mm. They are arranged parallel to each other, with each tube positioned 30 mm from the lead layer. The connection between the two GMC systems operates on a coincidence basis. Due to the system's high current consumption, it necessitates a battery with substantial capacity to facilitate continuous real-time outdoor measurements. Consequently, the system is designed to utilize a high-capacity battery of 15000 mAh, sufficient for one day of operation. Additionally, it incorporates a solar panel for battery recharging. The design of the enclosure also includes a cooling fan to mitigate the internal temperature rise caused by the heat generated from continuous operation of the components.

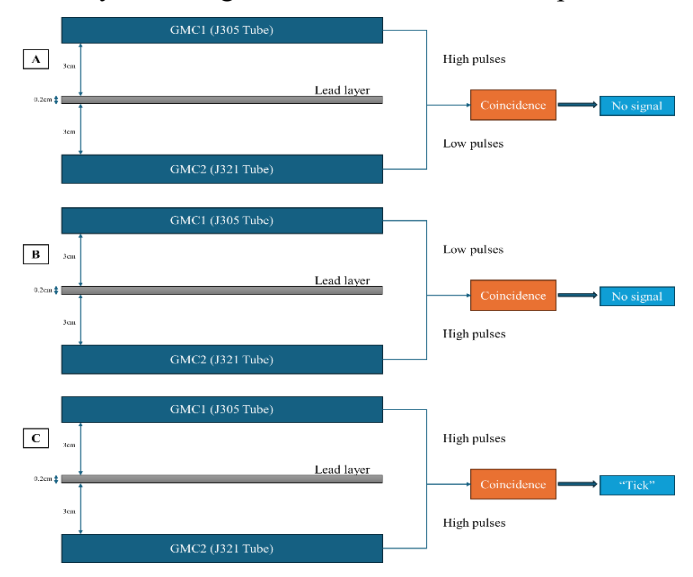


Figure 5. Schematic representation of valid and invalid coincidence events using a dual-tube GM setup

Figure 5A shows that the event only triggers GMC1 (J305); a particle passes through and only triggers the upper tube. The lower J321 tube does not receive a simultaneous pulse. Then, there is no coincidence event; the coincidence circuit does not record. Similarly, in Figure 5B, the particle passes through GMC2 (J321), is stopped by the lead layer, and activates only the lower tube. It leads to no coincidence conditions. With Figure 5C, a cosmic particle (e.g., muon) passes through both tubes almost simultaneously, both GMs emit pulses within a very short "coincidence window" (~µs), the coincidence circuit registers the event, and the "tick" is the sound from the buzzer or LED on coincidence circuit notice for a valid muon is recorded. This is the exact operating principle of the muon coincidence measurement system by using the GMC method. Coincidence eliminates noise events (background, nondirectional gamma rays) and only records particles with a known direction, such as cosmic muons. The event only occurs in case C, when both GM tubes record a pulse almost simultaneously. Using the J305 and J321 GMC tubes system allows for signal coincidence testing with two different types of tubes to compare performance, which makes the configuration mimic "a telescope-style" detection system by aligning two GM tubes for angular selection (Rossi, 1964). The outdoor setup of the system is described in Fig.6:



Figure 6. Outdoor system setup

### 3.1.3. Solid angle

In a coincidence-based muon detection system, the view field is defined by the geometric configuration of the GM tubes. When two cylindrical detectors are aligned vertically and separated by a fixed distance, they form a limited angular acceptance for incident particles. Only particles traveling along trajectories that intersect both tubes within a narrow time window are counted as valid events. The effective solid angle ( $\Omega$ ) is a measure of the detector's directional sensitivity. The solid angle subtended by the system can be approximated using the equation (2) (Braibant et al., 2012):

$$\Omega = 4 \times \sin^{-1} \left( \frac{lb}{\sqrt{(l^2 + 4d^2)(b^2 + 4d^2)}} \right), \tag{2}$$

where *l* is the length of the tubes, *b* is the width (diameter), and *d* is the semi-distance.

# $\Omega \approx 0.507 \, \mathrm{sr}$ Area A $\approx 0.51 \, \mathrm{cm^2}$ $\phi \approx 9.46^\circ$ Detector

# Solid Angle Visualization ( $\Omega \approx$ 0.5065 sr)

Figure 7. The visualize of solid angle

Figure 7 visually simulates the solid angle  $(\Omega)$  that a GM coinciding measuring system can record. The red cone represents the spatial view field of the system, i.e., the space through which a particle must pass in order to be simultaneously recorded by the two detector tubes. The tip of the cone is the location of the measuring system (detector), represented by the blue cube at the origin. The edge of the cone forms an opening angle  $\phi$  with respect to the principal axis (vector r), which is the spatial opening semi-angle of the measuring system; this angle is defined as equation (3):

$$\phi = \arctan\left(\frac{b}{2d}\right),\tag{3}$$

where b is the width (diameter), and d is the semi-distance. The edge of the cone forms an opening angle  $\phi \approx 9.46^{\circ}$ .

The circular surface on the top of the cone (*A*) is the area that the system can "capture" on the unit sphere, by using formula (4) (Born, 2013):

$$A = \Omega \times r^2,\tag{4}$$

with r = 1 as the normalized radius of the sphere. From geometry, the solid angle  $\Omega \approx 0.5065$  sr (steradian). Correspondingly, the projected area on the sphere is  $A \approx 0.51$  cm<sup>2</sup>.

### 3.2. Experimental setup

A dual-detector coincidence system was built and placed in an open outdoor setting to measure the cosmic ray muon flux in relation to the zenith angle. Two separate GM1 and GM2

tubes are part of the configuration; each is outfitted with J305 and J321 tubes. The two counters are positioned in parallel, 60 mm apart (30 mm from the lead surface to each tube), and separated by a 3 mm thick lead shielding. A movable stand supports the system, enabling accurate angle adjustments of 0° (vertical), 30°, 45°, 60°, and 90° (horizontal). The system is shown in **Figure 8**:

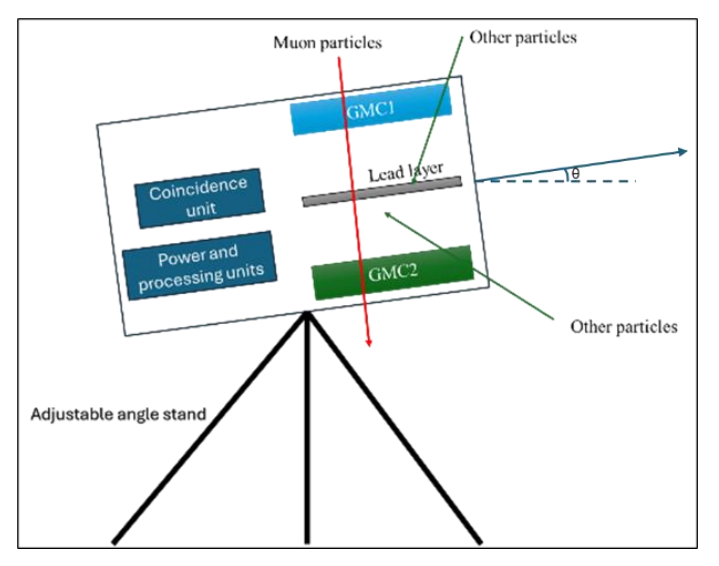


Figure 8. Illustrating a schematic setup for detecting cosmic ray muons using two GM counters (GMC1 and GMC2), which aligns with your experiment to evaluate muon flux as a function of the zenith angle

Three different kinds of count data are gathered:

- GMC1: GM tube upper raw counts (J305)
- GMC2: GM tube lower raw counts (J321)
- Coincident value (CV): When muons flow through both tubes at the same time, there are valid coincidence counts between GM1 and GM2.

This work developed two evaluation metrics, the Directional Index (DI) and the Noise Rejection Ratio (NRR), to better examine muon detection performance beyond traditional count rates. The ratio of legitimate coincidence events to all non-coincidence detections is known as the NRR, and it can be mathematically stated in equation (5):

$$NRR = \frac{N_{coincidence}}{N_{GMC1} + N_{GMC2} - 2N_{coincidence}},$$
(5)

where  $N_{coincidence}$  is the number of coincidence events measured,  $N_{GMC1}$  and  $N_{GMC2}$  are the number of each GMC counted.

This parameter shows the way the lead-shielded coincidence setup works by directly measuring the system's capacity to suppress background noise and non-muon events. A higher NRR strengthens the system's dependability for cosmic ray measurements in outdoor settings by indicating that it captures a greater percentage of real muon events.

To quantify the degree of concordance between the experimental muon flux angular distribution and the theoretical model, this study introduces an index termed the Directional Index (DI). This index is constructed based on the classical model, where represents the muon flux at zenith angle, and denotes an exponent characterizing the angular selectivity of the

measurement system (Grieder, 2001). In essence, DI is built on the concept of normalizing the experimental muon flux to the value at  $0^{\circ}$  angle, and then comparing it with the corresponding normalized theoretical distribution from the model. A DI value approaching 1 indicates superior model agreement, whereas a lower value suggests potential deviations arising from the uneven performance of the instrument, angular error, or the influence of background noise. Unlike the single regression method, which solely provides the exponent n value, the DI index offers a comprehensive assessment of the measurement system, encompassing orientation selectivity and angular distribution accuracy. This is the rationale for proposing the DI index in this study as a novel quantitative support tool, particularly beneficial for low-cost muon measurement systems that have not yet achieved the high accuracy of dedicated detectors. It is calculated as equation (6):

$$DI = \frac{\sum_{\theta} N_{coincident}(\theta) \times \cos^{n}(\theta)}{\sum_{\theta} N_{coincident}(\theta)},$$
(6)

where  $\sum_{\theta} N_{coincident}(\theta)$  total number of valid muon events recorded at all angles.

The degree to which the actual muon flux matches the anticipated angular dependence is shown by this index. Substantial directional conformance and slight systematic inaccuracy in angular alignment are indicated by a score of around one. When combined, these two metrics offer a more thorough understanding of the detection system's precision and resilience. They could be used as common standards for the next inexpensive cosmic ray research.

Average temperature (°C)	Height about the sea level (m)	Average air pressure (hPa)
$30.25 \pm 0.05$	$9.0 \pm 0.1$	$1006 \pm 1$

Table 1. Environmental conditions at the measurement site

Table 1 is the conditions monitored at the measurement site. Temperature, altitude, and air pressure are among the additional characteristics that must be tracked by thermometers, manometers, and altimeters in order to guarantee the best possible gadget operation. Temperature will alter the pulse threshold by affecting the breakdown voltage in the GM tube, which the manufacturer states should not exceed 40°C. The gas inside is more readily ionized at high temperatures, which might lengthen the dead period or accelerate spurious pulses. In the absence of cooling, electronic circuits (amplifiers, overlapping logic) may also deviate slightly from the reference value. Air pressure is directly impacted by air pressure, which modifies the air's muon energy loss rate. Because muons must travel through a thinner layer of the atmosphere at low pressure, there is a minor increase in the number of muons that reach the Earth. The protective atmosphere becomes thinner at higher altitudes, which causes the number of muons to increase significantly.

### 4. Results and discussion

### 4.1. Muon detection per zenith angle

In the Figure 9, the raw counts of each tube are displayed in the GMC1 and GMC2 columns with the value at the left axis. The count of GMC2 is regularly larger than that of GMC1 by using the different GM tubes. Coincidence curve in right axis, clearly shows the declining trend of the muon count traveling through the two tubes, decreasing from 484 to 47 as the zenith angle increases from  $0^{\circ}$  to  $90^{\circ}$ .

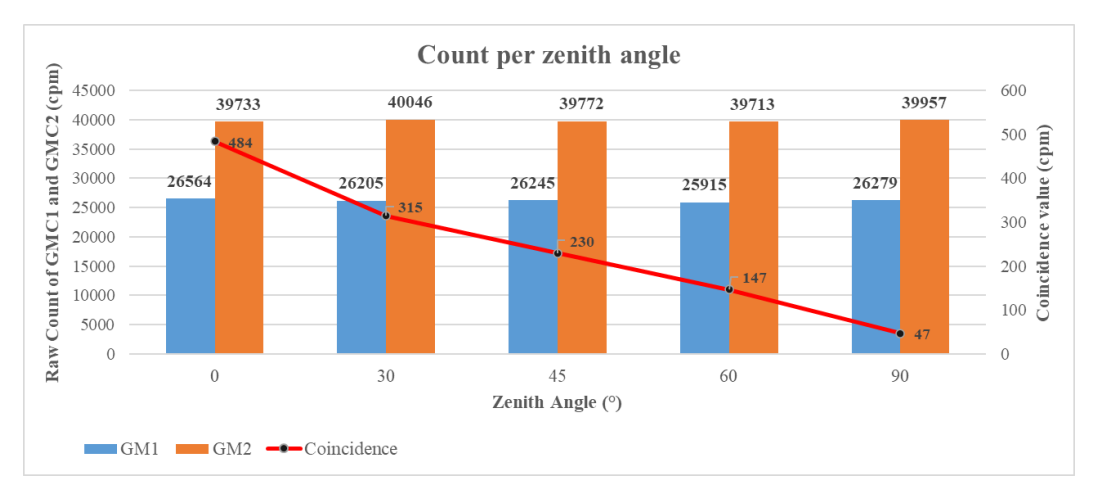


Figure 9. The raw counts of GMC1, GMC2, and CV collected

To evaluate the relative contribution of each GMC to the total number of valid coincidence events, two normalized ratios were calculated: Rate 1 and Rate 2. These ratios represent the proportion of coincidence counts relative to the total counts from GMC1 and GMC2, respectively. They are defined as both equation (7) and (8):

$$Rate \ 1 = \frac{CV}{GMC1},\tag{7}$$

$$Rate \ 2 = \frac{cv}{GMC^2},\tag{8}$$

which GMC1 and GMC2 are the total counts per minute (cpm) that the upper and lower GM tubes recorded, and CV is the number of coincidence events. The effective contribution and sensitivity of each tube in detecting legitimate muon events can be compared upon these rates given as percentages. A markedly unbalanced rate could be a sign of differences in shielding effects, detector alignment, or efficiency.

To quantify the directional muon flux at each zenith angle, the following expression was employed as equation (9):

$$\Phi_{\rm d} = \frac{cV}{A \times t \times \Omega},\tag{9}$$

where A is the effective detection area of the GM coincidence system (in cm²), CV is the number of valid coincidence counts recorded over the duration t,  $\Omega$  is the solid angle subtended by the geometry of the two-tube setup (in steradians), and  $\Phi_d$  is the muon flux in units of muons per square centimeter per second per steradian (muons/cm²/s/sr). A normalized comparison of flux levels across various zenith angles is made possible by this formulation, which takes into consideration the detector system's geometrical and temporal acceptance. By ensuring that only muons traveling through both tubes are taken into account, the CV successfully eliminates background noise. The actual directional muon intensity reaching the Earth's surface is consequently reflected in the computed flux values.

Table 2 summarizes the calculated detection efficiency and muon flux at various zenith angles based on the coincidence measurement data. The parameters Rate 1 and Rate 2 represent the proportion of coincidence events relative to the total counts recorded by the upper (GM1) and lower (GM2) GM tubes, respectively. As expected, both rates show a monotonic

decrease as the zenith angle increases, with Rate 1 decreasing from 1.82% at 0° to 0.18% at 90°, and Rate 2 from 1.22% to 0.12%. This reduction indicates that the effective detection probability diminishes significantly for more oblique angles, consistent with geometric attenuation and muon decay in the atmosphere.

Table 2. Coincidence rates and directional flux at various zenith angles. Flux in muons/cm²/min

Zenith angle	Rate 1 (%)	Rate 2 (%)	Directional muon flux $(\Phi_d, muon/cm^2/s/sr)$	Muon flux (Φ, muon/cm²/min)
0	1.822015	1.218131	0.021686	1.301
30	1.202061	0.786595	0.014114	0.847
45	0.876357	0.578296	0.010305	0.618
60	0.567239	0.370156	0.006586	0.395
90	0.17885	0.117626	0.002106	0.126

The number of muons per unit area, per second, and per unit solid angle is represented by the directional muon flux  $\Phi_d$ , which is computed using the equation (9). At 0°, the measured value is roughly 0.0217 muons/cm²/s/sr, which, when converted, equals 1.301 muons/cm²/min. The correctness of the apparatus and its calibration is confirmed by this result, which closely matches the typical theoretical muon flux at sea level, about 1 muon/cm²/min for vertical incidence (Axani et al., 2017).

### 4.2. Zenith angle influence on count rate

To evaluate the angular conformity of the experimental muon flux data to the theoretical model, a Bayesian approach using Markov Chain Monte Carlo (MCMC) sampling was employed (Gelman et al., 2013). The directional flux of muons is known to follow the power-law dependence. As equation (1), where  $N(\theta)$  is the number of valid muon events recorded at zenith angle  $\theta$ , and n is the angular exponent to be estimated, as shown in Table 3.

Table 3. Value of cos²(θ) and Normalize Coincidence number to value at 0° based on each zenith angle

Zenith angle (°)	cos²(θ)	Normalize Coincidence number to value at 0°	
0	1	1.0000	
30	0.75	0.6508	
45	0.5	0.4752	
60	0.25	0.3037	
90	0	0.0971	

Normalized coincidence counts at five zenith angles with values:

- x = [1.0, 0.75, 0.5, 0.25, 0].
- y = [1.0000, 0.6508, 0.4752, 0.3037, 0.0971].

The MCMC result yielded  $n = 1.063 \pm 0.107$ 

With an exponent somewhat smaller than the conventional n = 2, which is theoretically expected under ideal air conditions, the result confirms a cosine-based angular dependency of the muon flux.

Experimental constraints such as angular misalignment, background noise, or systematic errors at greater zenith angles could be the cause of this discrepancy. However, the Bayesian estimation shows that the experimental data closely resemble the expected directional behavior of cosmic ray muons.

### 4.3. System performance analysis

The NRR is determined by calculating the percentage of valid coincidence counts relative to all recorded counts, thereby assessing the system's ability to suppress background noise and non-muon events. This calculation utilizes the total counts from the GMC1 and GMC2 Geiger-Müller counters, as well as the legitimate coincidence events from each perspective.

$$NRR \approx 0.00373$$

This indicates that only about 0.373% of all detected events were true muon coincidences, emphasizing the importance of the coincidence circuit in filtering out environmental and electronic noise. To assess how well the experimental data's angular distribution fits the theoretical model  $N(\theta) = N(0^{\circ}) \cdot \cos^{n}(\theta)$ , where the exponent n was previously found to be  $1.063 \pm 0.107$  using Bayesian MCMC sampling, the DI is calculated as:

$$DI \approx 0.804$$

The calculated DI was approximately 0.804, suggesting that the observed angular distribution of muon flux aligns well with the expected theoretical dependence. This value reflects a relatively strong directional sensitivity, validating the geometrical configuration and effectiveness of the detection system.

### 4.4. Discussion

The measured angular dependence of muon flux exhibits qualitative agreement with the expected  $\cos^2\theta$  model, though the fitted exponent  $n=1.063\pm0.107$  indicates a significant deviation from the ideal case. This discrepancy likely stems from systematic uncertainties and limitations in alignment, background noise or shielding.

The absorption and decay properties of muons in the atmosphere are reflected in the abrupt drop in coincidence counts as the zenith angle increases from 0° to 90°. Around the theoretical standard value at sea level, approximately 1 muon/cm²/min, the muon flux at 0° angle is approximately 1,301 muons/cm²/min.

With a NRR of equal 0.373% or so, the bulk of the events recorded were either non-muons or background noise. But this also demonstrates how crucial and successful the coincidence circuit is in removing real muon occurrences. The low NRR value is normal for open outdoor GM instruments. The DI = 0.804 suggests partial alignment with the expected angular distribution. However, it also reflects deviation mostly attributed to geometric misalignment, background fluctuations, or tube efficiency mismatches. It proves that the

measurement system, device configuration, as well as the angular calibration procedure are performed correctly and reasonably.

### 5. Conclusion

The observations are in accordance with the  $\cos^2\theta$  theoretical model, and the experimental results validate the angular dependence of cosmic ray muon flow. The detection results were dependable and statistically consistent, utilizing a low-cost, outdoor GM coincidence system. Expected muon decay and air attenuation are reflected in the notable decrease in coincidence counts at greater zenith angles. By employing a coincidence circuit and lead shielding, the device was able to effectively separate muon signals from background radiation. Additionally, a more sophisticated evaluation of detection effectiveness and directional accuracy was made possible by adding NRR and DI measures. The results demonstrate that significant cosmic ray research may be carried out with high fidelity even with few resources, paving the way for easily accessible educational experiments and the advancement of reasonably priced muon detection equipment.

**Acknowledgements:** We acknowledge Ho Chi Minh City University of Technology (HCMUT), VNU-HCM for supporting this study.

### References

- Arcani, M., Rossi, L., & Peluso, S. (2024). Transforming DIY Geiger counter kits into muon detectors for education and scientific exploration. *Journal of Instrumentation Education and Physics*, 19(2), 112–120.
- Axani, S. N., Conrad, J. M., & Kirby, C. (2017). The desktop muon detector: A simple, physics-motivated machine-and electronics-shop project for university students. *American Journal of Physics*, 85(12), 948–958.
- Bae, G., Kim, J., & Choi, H. (2021). Effective solid angle model and Monte Carlo method: Improved estimations to measure cosmic muon intensity at sea level in all zenith angles. *Astroparticle Physics*, *135*, 102620.
- Borja, C., Ávila, C., Roque, G., & Sánchez, M. (2022). Atmospheric muon flux measurement near Earth's equatorial line. *Instruments*, 6(4), 78. https://doi.org/10.3390/instruments6040078
- Born, R. (2013). *Determining the efficiency of a Geiger–Müller tube*. Vernier Software & Technology. Available from <a href="https://www.vernier.com/files/innovate/determining\_the\_efficiency\_of\_a\_geiger-mueller-tube.pdf">https://www.vernier.com/files/innovate/determining\_the\_efficiency\_of\_a\_geiger-mueller-tube.pdf</a>
- Braibant, S., Giacomelli, G., & Spurio, M. (2012). *Particles and fundamental interactions: An introduction to particle physics*. Springer.
- CAEN S.p.A. (2023). *Zenith angle dependence of muon flux*. CAEN Educational Resources. Available from https://edu.caen.it/app-note/zenith-angle-dependence-of-muon-flux/
- CERN. (2023). *Cosmic rays: Particles from outer space*. Available from https://home.cern/science/physics/cosmic-rays-particles-outer-space
- Cox, S. F. J. (2009). Muonium as a model for hydrogen in materials. *Reports on Progress in Physics*, 72(11), 116501. https://doi.org/10.1088/0034-4885/72/11/116501
- Gaisser, T. K. (1990). Cosmic rays and particle physics. Cambridge University Press.

- Gelman, A., Carlin, J. B., Stern, H. S., Dunson, D. B., Vehtari, A., & Rubin, D. B. (2013). *Bayesian data analysis* (3<sup>rd</sup> ed.). CRC Press.
- Grieder, P. K. F. (2001a). Cosmic ray properties, relations and definitions. In *Cosmic rays at Earth* (Ch. 1, p. 25). Elsevier.
- Grieder, P. K. F. (2001b). Cosmic rays in the atmosphere. In *Cosmic rays at Earth* (Ch. 2, p. 102). Elsevier.
- Grieder, P. K. F. (2001c). Cosmic rays at sea level. In *Cosmic rays at Earth* (Ch. 3, p. 432). Elsevier.
- Hughes, V. W., & Kawall, D. (2001). The muon g-2 experiment. *Annual Review of Nuclear and Particle Science*, 51, 341–389. https://doi.org/10.1146/annurev.nucl.51.101701.132446
- Massachusetts Institute of Technology. (2015). *Geiger–Müller counter circuit theory* [Course materials]. MIT OpenCourseWare. Available from https://ocw.mit.edu/courses/22-s902-do-it-yourself-diy-geiger-counters-january-iap-2015
- McKenna, P. (2021, May 28). DIY muon tomography. *IEEE Spectrum*. Available from https://spectrum.ieee.org/diy-muon-tomography
- Nagamine, K. (2003). Introductory muon science. Cambridge University Press.
- Particle Data Group. (2020). Review of particle physics. *Progress of Theoretical and Experimental Physics*, 2020(8), 083C01. https://doi.org/10.1093/ptep/ptaa104
- Rossi, B. (1964). Cosmic rays. McGraw-Hill.